Hindawi
Mathematical Problems in Engineering
Volume 2019, Article ID 2130617, 7 pages
https://doi.org/10.1155/2019/2130617

Research Article

A Theoretical Model for the Rake Blockage Mitigation in Deep Cone Thickener: A Case Study of Lead-Zinc Mine in China

Zhuen Ruan,[1] Yong Wang ,[1,2] Aixiang Wu ,[1] Shenghua Yin,[1] and Fei Jin[1]

[1]*School of Civil and Resource Engineering, University of Science and Technology Beijing, Beijing 100083, China*
[2]*State Key Laboratory of Coal Resources and Safe Mining, China University of Mining and Technology, Xuzhou 221116, China*

Correspondence should be addressed to Yong Wang; wangyong8551@126.com

Received 16 September 2018; Accepted 6 January 2019; Published 22 January 2019

Academic Editor: Isabel S. Jesus

Deep cone thickener (DCT) is key equipment in cemented paste backfill (CPB) technology. However, rake blockage occurs frequently in DCT during the dewatering process of the unclassified tailings being thickened from dilute slurry to thickened tailings or paste. Rake blockage has disastrous effects on the CPB operation. In order to investigate the influencing factors of rake blockage in DCT, a mathematical model of rake power in DCT was developed. In addition, stacking mud bed (made of thickened tailings) from the DCT in Huize lead-zinc mine (HLZM) in different rake blockage accidents was sampled and tested to investigate the effect of tailings characters on rake blockage. Results indicated that the concentration of the mud bed and the friction between the mud bed and the cone wall contributed to the rake blockage. The concentration and friction were influenced by the high content of coarse particles in the mud bed. Moreover, activating devices for bed mud, as the corrective and preventive action, were developed to prevent the rake blockage, which was valid in HLZM.

1. Introduction

Millions of tons of ore are processed annually to meet the economic demand and social development, accompanied with unprecedented worrying of the accumulation and increment of solid waste (waste rock or tailings) [1]. Therefore, disposal or utilization of tailings is of great importance for both environmental [2] and economic reasons [3]. With the development of cemented paste backfill (CPB), unclassified tailings in the mining industry are widely used for subsidence control [4–7], solid waste management [8–10], and water conservation and reuse in mine [11, 12]. The deep cone thickener (DCT) that produces a high concentration underflow is employed to consolidate the unclassified tailings from a dilute slurry to thickened tailings [13, 14], which is the key to CPB [15, 16].

Rake is essential for DCT, which produces 'drainage channel' for transporting water from the bottom to the up and transports the sediment bed material to the underflow [17–19]. Using laboratory experiments and numerical simulation, many studies focused on the influence on thickening performance, rake torque calculation, and rake design. Albertson [20] established a mathematical model for calculating the transport capacity of rakes, which improved the rakes design. Wu et al. [21] analyzed the influence of the rake rod number and rake rod arrangement on the thickening behavior with a laboratory experiment. Based on CFD simulation, Šutalo et al. [22] observed the flow patterns around rakes, while Huang et al. [23] and Ruan et al. [24] investigated the influence of rotation speed and rake structure on thickening. Rake torque is a key parameter in DCT design and operation which is mainly influenced by the yield stress of the suspension [17]. To produce high concentration underflow, the yield stress of underflow in DCT is much higher than conventional high-rate thickeners, resulting in a much higher rake torque demanding for DCT [25]. The yield stress of the suspension, rotation speed, and rake structure have great influence on rake torque [26]. Wu et al. [27] proposed a torque model for complex structure rakes based on the influence of slurry concentration on rake and height of the bed. Tan et al. [28] formulated a rake torque model as a function of solids concentration, which pays more attention to underflow solids concentration rather than rheological properties and overcomes the shortcomings of yield stress measurements.

Nevertheless, the influence of aggregate densification [29, 30] is not considered in this work. On the basis of structural characteristics of aggregation network and initial shear stress of high concentration slurry, Wang et al. [31] proposed a torque mathematical model to predict the rake torque increase with an increase in underflow concentration and bed height during DCT operation. Recently, Li et al. [32] tried to analyze the rake blockage in DCT with dynamic sedimentation test and rheological parameters measurement, concluding that the rake blockage is mainly caused by the change of slurry rheological parameters as a result of the intermittent operation.

Although many studies have been conducted for rakes in DCT, very few studies of rake blockage have been published. Generally, rake blockage occurs frequently in DCT whether it is an intermittent or continuous operation because of the high concentration and yield stress, which has disastrous effects on the CPB operation. Huize lead-zinc mine (HLZM), Chihong Zn & Ge Co., Ltd, is the first mine in China to use CPB technology successfully since 2006. However, rake blockage, which is one of the main challenges faced, occurs 26 to 36 times every year, affecting the normal operation of the CPB system seriously [33, 34].

Therefore, this work tried to advance our understanding of influencing factors of rake blockage in DCT. A theoretical model for the power of DCT was proposed that considers the effect of density of mud bed, friction coefficient, the rotation speed of rakes, and the cone angle of DCT. Based on the model, the effect of tailings characters on rake blockage in HLZM was investigated, with tacking mud bed (made of thickened tailings) from the DCT in different rake blockage accidents sampled and tested. Furthermore, a corrective and preventive action was proposed. A set of activating devices for bed mud was established to prevent the rake blockage, which was valid in HLZM.

2. Materials and Methods

2.1. Total Tailings Property of HLZM. The true density of total tailings from HLZM is 2.75 g/cm^3, measured by the pycnometer test method. The corresponding bulk density is 1.75 g/cm^3, measured by the weight method. As a result, the porosity was calculated as 36.36%. Standard sieves and laser particle size analyzer (LMS-30) were employed for analysis of the particle size distribution (PSD) of tailings of +200 mesh (>75 μm) and -200 mesh (≤75 μm), respectively. The average particle size is 75.59 μm and the median particle size is 34.95 μm. The specific surface area is 1685 cm^2/cm^3. In addition, the content of >100 μm and ≤20 μm is 20% and 37.20%, respectively. The PSD curve is shown in Figure 1. Oxidized tailings and sulfide tailings are the main tailings products during the mineral separation in HLZM. The chemical composition analysis on micronized tailings was performed by X-Ray Fluorescence (XRF) and Atomic Absorption Spectrometer (AAS), which is given in Table 1. It can be seen that the oxidation rates of Zn and Pb are 80% and 92%, respectively.

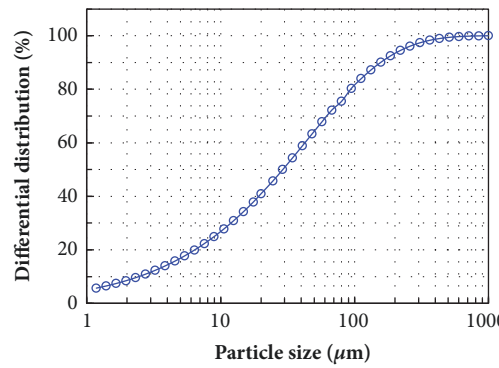

Figure 1: The particle size distribution of total tailings.

Table 1: Chemical composition of the tailings.

Chemical composition	Content %
ZnO	2.29
Zn	1.88
PbO	0.63
Pb	0.59
S	0.58

2.2. Concentration and Particle Size Distribution Analysis. To investigate the effect of tailings characters on rake blockage, stacking mud bed under the rakes of 6 rake blockage accidents in HLZM in 2011 was sampled and tested. The concentration of the tailings was measured by the oven drying method. The content of particles coarser than 200 mesh was analyzed by standard sieves.

2.3. Power Theoretical Model for DCT. Rakes are the component of DCT that rotate through the density slurry and mechanically scrape the solids to the underflow discharge point and thus provide a dewatering effect. The rakes are powered by the DCT drive mechanism and connected to the drive by a shaft, as shown in Figure 2(a). When the mud bed on the cone wall is stacked up, the rakes cannot rotate, such that rake blockage happens. As shown in Figure 2(b), R_0 is the radius of DCT and r_0 is the distance between the point where the stacking mud bed is the thickest and the shaft. It must be noticed that r_0 has a positive correlation with the capacity of DCT and the concentration of unclassified tailings [35].

In this paper, linear distribution of the thickness of stacking mud bed was made as an assumption. As shown in Figure 3, a differential element $(dy, d\beta)$ is taken from the stacking mud bed. y_0 represents the effective height of rakes and α is the cone angle of DCT. The mass of the differential element is

$$\begin{aligned} dm &= \rho \cdot dV = \rho \cdot \left(r_0 - \frac{r_0 \cdot y}{y_0}\right) \cdot r \cdot dy \cdot d\beta \\ &= \rho \cdot r_0 \left(1 - \frac{y}{y_0}\right) \cdot r \cdot dy \cdot d\beta, \end{aligned} \tag{1}$$

where ρ is the density of the differential element, and (r, y) is the coordinate on the XY plane.

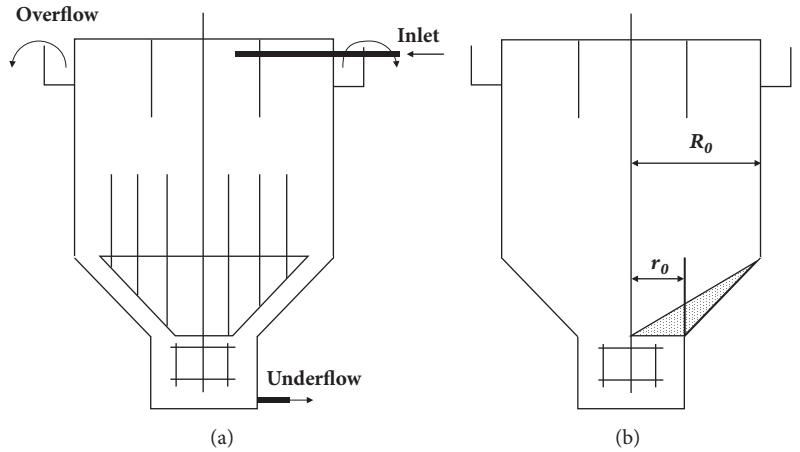

Figure 2: Sketch of (a) DCT and (b) stacking mud bed.

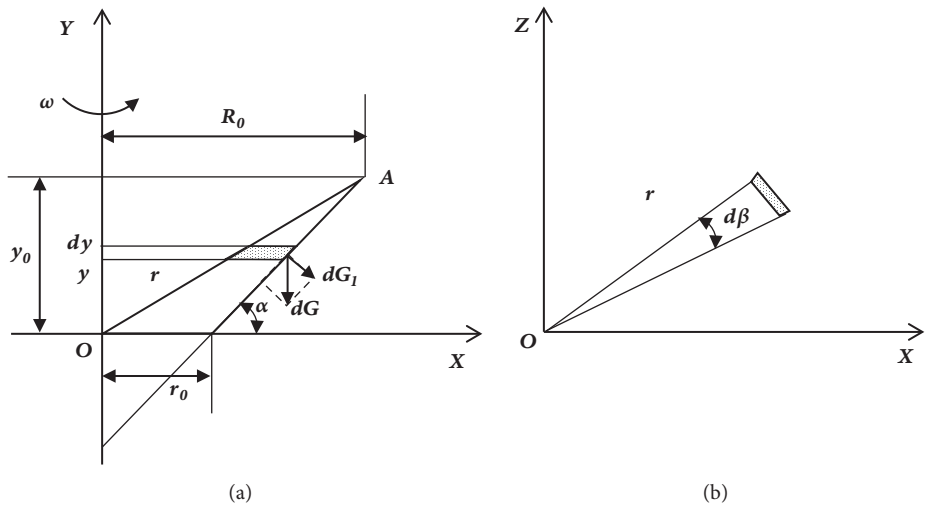

Figure 3: Force analysis of rake in DCT: (a) front view and (b) vertical view.

The component force perpendicular to the cone wall of gravity is

$$\begin{aligned} dG_1 &= g \cdot d_m \cdot \cos\alpha \\ &= \rho \cdot g \cdot r_0 \cdot \cos\alpha \cdot \left(1 - \frac{y}{y_0}\right) \cdot r \cdot dy \cdot d\beta, \end{aligned} \tag{2}$$

where g is the acceleration of gravity.

During the rotation, the rake should overcome the friction between stacking mud bed and the cone wall to rotate and scrape the solids. The friction is

$$\begin{aligned} dF &= \mu \cdot dG_1 \\ &= \mu \cdot \rho \cdot g \cdot r_0 \cdot \cos\alpha \cdot \left(1 - \frac{y}{y_0}\right) \cdot r \cdot dy \cdot d\beta, \end{aligned} \tag{3}$$

where μ is the friction coefficient.

The power source for rakes in DCT is the drive head or tractor. The driving power for the differential element is

$$\begin{aligned} dP &= R \cdot dF \cdot \omega \\ &= \mu \cdot \rho \cdot g \cdot r_0 \cdot \omega \cdot \cos\alpha \cdot \left(1 - \frac{y}{y_0}\right) \cdot r^2 \cdot dy \cdot d\beta, \end{aligned} \tag{4}$$

where ω is the rotation speed of rakes.

The geometrical relationship between r and y can be found in Figure 2(b) as

$$r = r_0 + \frac{R_0 - r_0}{y_0} \cdot y. \tag{5}$$

Inserting (5) into (4), the driving power can be written as

$$\begin{aligned} dP = \mu \cdot \rho \cdot g \cdot r_0 \cdot \omega \cdot \cos\alpha \cdot \left(1 - \frac{y}{y_0}\right) \\ \cdot \left(r_0 + \frac{R_0 - r_0}{y_0} \cdot y\right)^2 \cdot dy \cdot d\beta. \end{aligned} \tag{6}$$

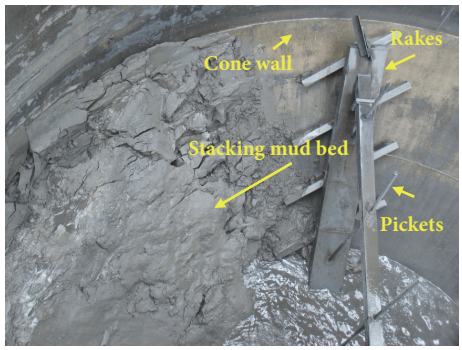

Figure 4: Rake blockage in HLZM (2011).

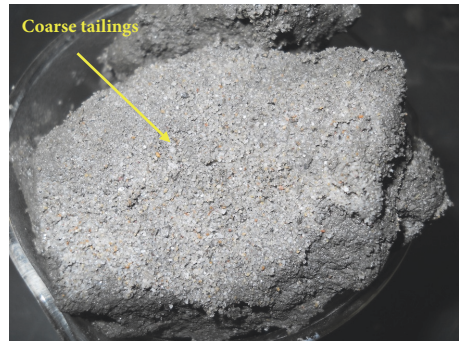

Figure 5: Coarse particles in stacking mud bed (filter cake).

In general, μ, ρ, g, r_0, ω, and α do not change with y and β. At the same time, $y_0 = (R_0 - r_0) \cdot \tan\alpha$. Integrate (6) and get the total driving power as

$$P = \frac{1}{6}\pi \cdot \mu \cdot \rho \cdot g \cdot \omega \cdot \sin\alpha \cdot \left(-3{r_0}^4 + R_0 \cdot {r_0}^3 + {R_0}^2 \cdot {r_0}^2 + {R_0}^3 \cdot r_0\right). \quad (7)$$

3. Results and Discussion

Usually, when the total driving power exceeds the rated power, rake blockage occurs; otherwise, rakes rotate normally. It can be concluded from (7) that the physicochemical property of tailings, structure and rotation speed of rakes, and the capacity of DCT are the critical factors contributing to rake blockage. Since $-3{r_0}^4 + R_0 \cdot {r_0}^3 + {R_0}^2 \cdot {r_0}^2 + {R_0}^3 \cdot r_0 \geq 0$ is always true because of $0 \leq r_0 \leq R_0$, the total driving power P is proportional to μ, ρ, ω, and α. When the value of one or more of them is too large, the rake blockage will happen. R_0 and r_0 are constant and vary with the capacity of DCT and the concentration of unclassified tailings, respectively, so their influence on total driving power is mainly caused by r_0. The changes of μ, ρ, ω, α, and r_0 that caused rake blockage and corrective and preventive action are analyzed and discussed in the following subsections.

3.1. The Effect of Friction Coefficient. The particle size influences the friction coefficient between the flowing slurry and wall [36, 37]. The friction coefficient of coarse particles is always larger than that of fine particles. During 2006 and 2011, 154 rake blockage accidents happened in the DCT in HLZM. The stacking mud bed was filter cake (Figure 4). The PSD of the stacking mud bed in 5 rake blockage accidents that happened in 2011 was analyzed (Table 2). Commonly, only when the coefficient of uniformity (C_u) and coefficient of curvature (C_c) meet the conditions $C_u \geq 6$ and $1 < C_c < 3$ can a sand be classified as well gradated and compacted [38, 39]. Moreover, the content of particles finer than 20μm in tailings paste slurry should be more than 15 % [40]. Nevertheless, the average distribution of particles coarser than 200 mesh (75 μm) was 57.56 %, which increased the friction coefficient dramatically.

Table 2: The content of particles coarser than 200 mesh in stacking bed.

Time	Particles (+200 mesh)
2011, April 15th	64.59 %
2011, April 21st	52.34 %
2011, August 14th	50.42 %
2011, August 16th	66.10 %
2011, August 20th	54.55 %

Table 3: Concentration and coarse particles (+200 mesh) in 5 samples.

Sample	Concentration	Particles (+200 mesh)
1	87.94 wt%	65.05%
2	87.33 wt%	65.46%
3	89.16 wt%	63.62%
4	81.58 wt%	65.47%
5	85.94 wt%	67.58%

3.2. The Effect of Density of Stacking Mud Bed. In general, concentration by weight is more popularly used than the density in CPB, so we substituted concentration for density. The statistical analysis showed that the concentration of stacking mud bed in 90% of the 154 rake blockage accidents was higher than the critical concentration (78 wt%) [33], resulting in the rake blockage directly. Five samples were taken from the stacking mud bed in another rake blockage accident on November 28, 2011. As shown in Table 3, the concentration lied between 81.58 wt% and 89.16 wt%, which is much higher than the critical value, while the average distribution of particles coarser than 200 mesh was 65.44 %, and the coarse particles in the stacking mud bed were shown in Figure 5. The specific surface area of particles varies with the particle size, resulting in different water-retaining characteristics. Typically, the coarser the particle is, the more specific the surface area is, and the less the sorptivity is, i.e., less water-retaining characteristics [41, 42]. Therefore, the high content of coarse particles in mud bed contributed to high concentration, i.e., density, resulting in the rake blockage.

As for ω, it was 0.176 r/min in HLZM, indicating that the rake rotated around the shaft quilt slowly. For the sake of

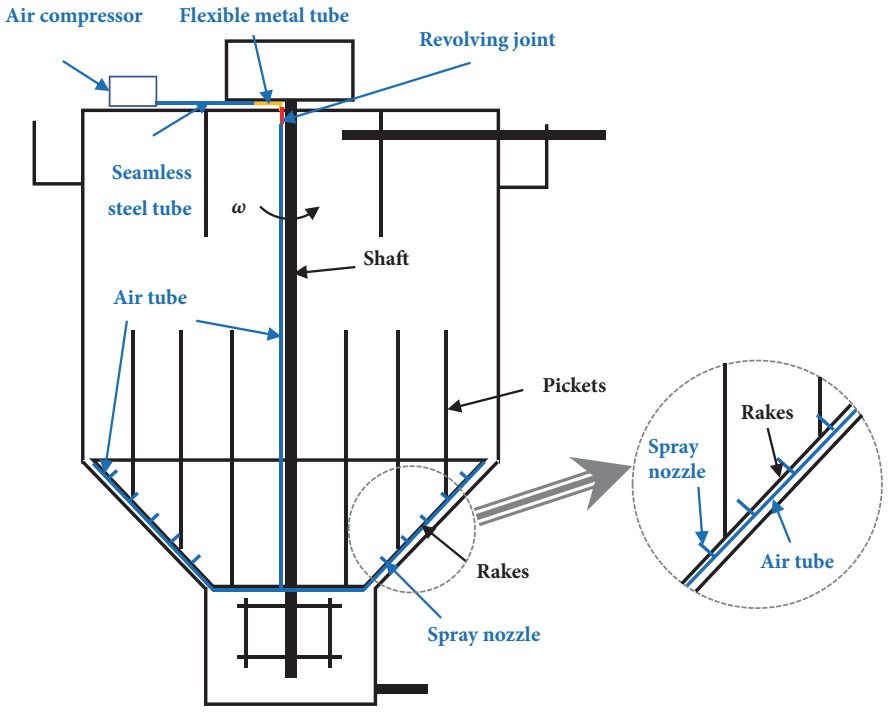

Figure 6: Sketch of activating devices for bed mud in DCT.

demand for underflow concentration, it cannot be transferred to a smaller value. At the same time, the α in HLZM is fixed. Therefore, the effect of ω and α on total driving power was not discussed. Nevertheless, they should be considered in other cases, like the new design for rake.

3.3. The Corrective and Improvement Measures for Rake Blockage. As discussed above, the PSD of mud bed, especially the high content of coarse particles with poor water-retaining characteristics, mainly contribute to rake blockage in HLZM. Because of the high local concentration and high friction between coarse particles and the cone wall, excessive local resistance in the cone was produced, resulting in frequent rake blockage accidents.

In order to prevent rake blockage, activating devices for bed mud, as the corrective and preventive action, were developed as shown in Figure 6. The seamless steel tube from air compressor was connected to the main air tube through the flexible metal tube and revolving joint on the top of DCT. The main air tube shared the same center axis with the shaft. In addition, 10 spray nozzles were fixed to the air cube which was fixed on the bottom of the rake. High-pressure gas billowed out from the spray nozzles will loosen the mud bed, improving the fluidity of the coarse particle swarm. At the same time, the concentration of the mud bed near the rake will be reduced. As a result, the rake torque was lowered and thus rake blockage was prevented.

In industrial production, it is difficult to monitor the total driving power. Instead, the rake torque is monitored to predict the rake blockage. Moreover, the relative torque to the rated rake torque was introduced to represent the rake

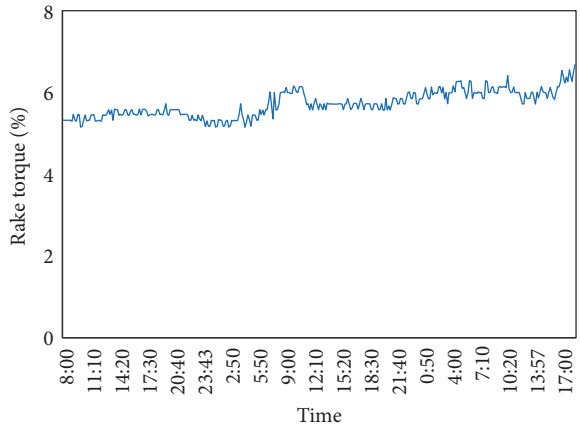

Figure 7: The rake torque in 58 hours in HLZM.

torque, and it is typically stated as a percentage. It was shown in Figure 7 that the rake torque was under 8%, which is much lower than the critical value of 60%. There has been no rake blockage in HLZM since 2015 (Figure 8), illustrating the activating devices for bed mud prevented the rake from blockage effectively.

4. Conclusions

Rake blockage is one of the main challenges faced in CPB. The mechanism and influencing factor of rake blockage in DCT were investigated in this paper. Stacking mud bed from the DCT in HLZM in different rake blockage accidents were sampled and tested. Further, a mathematical model of rake

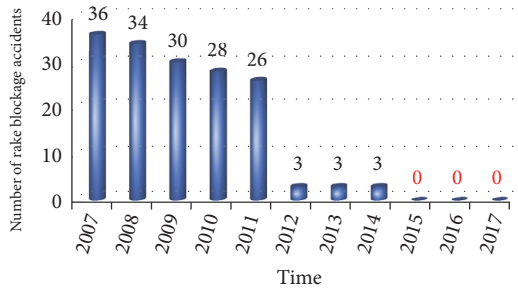

Figure 8: Number of rake blockage accidents in HLZM.

power in the DCT was developed. The main conclusions derived from this study are summarized as follows.

(1) The mathematical model of rake power was developed to investigate the influencing factors of rake blockage in the DCT. It was found that the density of stacking mud bed, the friction coefficient between mud bed and cone wall, the rotation speed of rakes, and the cone angle of DCT are the main influencing factors of the total driving power of rakes, which lead to blockage as it exceeds the rated value.

(2) The PSD of mud bed, especially the high content of coarse particles with poor water-retaining characteristics, is the main contribution for rake blockage in HLZM. Due to the high local concentration and high friction between coarse particles and cone wall, excessive local resistance in the cone was produced, resulting in the frequently occurring rake blockages.

(3) The activating devices for bed mud can effectively prevent the rake blockage in HLZM. With the high-pressure gas billowed out from the spray nozzles, the activating devices improve the fluidity of the coarse particle swarm and reduce the concentration of the mud bed near the rake, thereby lowering the rake torque.

Data Availability

The data used to support the findings of this study are available from the corresponding author upon request.

Conflicts of Interest

The authors declare that there are no conflicts of interest regarding the publication of this paper.

Acknowledgments

This research was funded by the National Natural Science Foundation of China (No. 51804015), the Research Fund of State Key Laboratory of Coal Resources and Safe Mining, CUMT (No. SKLCRSM18KF006), and the Fundamental Research Funds for the Central Universities (No. FRF-TP-17-024A1).

References

[1] C. Falagán, B. M. Grail, and D. B. Johnson, "New approaches for extracting and recovering metals from mine tailings," *Minerals Engineering*, vol. 106, pp. 71–78, 2017.

[2] C. Wang, D. Harbottle, Q. Liu, and Z. Xu, "Current state of fine mineral tailings treatment: A critical review on theory and practice," *Minerals Engineering*, vol. 58, pp. 113–131, 2014.

[3] B. Babel, M. Penz, E. Schach, S. Boehme, and M. Rudolph, "Reprocessing of a Southern Chilean Zn Tailing by Flotation—A Case Study," *Minerals*, vol. 8, no. 7, p. 295, 2018.

[4] L. Yang, J. Qiu, H. Jiang, S. Hu, H. Li, and S. Li, "Use of cemented super-fine unclassified tailings backfill for control of subsidence," *Minerals*, vol. 7, no. 11, p. 216, 2017.

[5] T. Belem and M. Benzaazoua, "Design and application of underground mine paste backfill technology," *Geotechnical and Geological Engineering*, vol. 26, no. 2, pp. 147–174, 2008.

[6] A. Wu, Y. Wang, and H. Wang, "Status and prospects of paste backfill technology," *Metal Mine*, vol. 45, pp. 1–9, 2016.

[7] Y. Wang, M. Fall, and A. Wu, "Initial temperature-dependence of strength development and self-desiccation in cemented paste backfill that contains sodium silicate," *Cement and Concrete Composites*, vol. 67, pp. 101–110, 2016.

[8] D. V. Boger, "Paste and thickened tailings - the way forward for a more sustainable mine waste management," *Ausimm Bulletin*, vol. 5, pp. 70–73, 2011.

[9] W. Sun, A. Wu, K. Hou, Y. Yang, L. Liu, and Y. Wen, "Experimental study on the microstructure evolution of mixed disposal paste in surface subsidence areas," *Minerals*, vol. 6, no. 2, p. 43, 2016.

[10] Y. Wang, A. Wu, Z. Ruan, H. Wang, Y. Wang, and F. Jin, "Temperature effects on rheological properties of fresh thickened copper tailings that contain cement," *Journal of Chemistry*, vol. 2018, Article ID 5082636, 8 pages, 2018.

[11] T. D. Toit and M. Crozier, "Khumani iron ore mine paste disposal and water recovery system," *Journal of the Southern African Institute of Mining and Metallurgy*, vol. 112, no. 3, pp. 211–220, 2012.

[12] A. J. Gunson, B. Klein, M. Veiga, and S. Dunbar, "Reducing mine water requirements," *Journal of Cleaner Production*, vol. 21, no. 1, pp. 71–82, 2012.

[13] M. J. Pearse, "Historical use and future development of chemicals for solid-liquid separation in the mineral processing industry," *Minerals Engineering*, vol. 16, no. 2, pp. 103–108, 2003.

[14] H. Jiao, A. Wu, H. Wang, S. Zhong, R. Ruan, and S. Yin, "The solids concentration distribution in the deep cone thickener: A pilot scale test," *Korean Journal of Chemical Engineering*, vol. 30, no. 2, pp. 262–268, 2013.

[15] D. Tao, B. K. Parekh, Y. Zhao, and P. Zhang, "Pilot-scale demonstration of deep cone™ paste thickening process for phosphatic clay/sand disposal," *Separation Science and Technology*, vol. 45, no. 10, pp. 1418–1425, 2010.

[16] A. Wu, Y. Wang, and H. Wang, "Estimation model for yield stress of fresh uncemented thickened tailings: Coupled effects of true solid density, bulk density, and solid concentration," *International Journal of Mineral Processing*, vol. 143, pp. 117–124, 2015.

[17] M. Rudman, K. Simic, D. A. Paterson, P. Strode, A. Brent, and I. D. Šutalo, "Raking in gravity thickeners," *International Journal of Mineral Processing*, vol. 86, no. 1-4, pp. 114–130, 2008.

[18] J. Du, R. A. Pushkarova, and R. S. C. Smart, "A cryo-SEM study of aggregate and floc structure changes during clay settling and raking processes," *International Journal of Mineral Processing*, vol. 93, no. 1, pp. 66–72, 2009.

[19] F. Schoenbrunn, "Dewatering to higher densitiesan industrial review," in *Proceedings of the 14th International Seminar on Paste and Thickened Tailings (Paste '11)*, pp. 19–23, Perth, Australia, 2011.

[20] O. E. Albertson and R. W. Okey, "Evaluating scraper designs," *Water Environment and Technology*, vol. 4, no. 1, pp. 52–58, 1992.

[21] A. Wu, Y. Wang, and H. Wang, "Effect of rake rod number and arrangement on tailings thickening performance," *Journal of Central South University*, vol. 45, no. 1, pp. 244–248, 2014.

[22] I. D. Šutalo, D. A. Paterson, and M. Rudman, "Flow visualisation and computational prediction in thickener rake models," *Minerals Engineering*, vol. 16, no. 2, pp. 93–102, 2003.

[23] G. Huang, J. Liu, L. Wang, and Z. Song, "Flow field simulation of agitating tank and fine coal conditioning," *International Journal of Mineral Processing*, vol. 148, pp. 116–123, 2016.

[24] Z.-E. Ruan, C.-P. Li, and C. Shi, "Numerical simulation of flocculation and settling behavior of whole-tailings particles in deep-cone thickener," *Journal of Central South University*, vol. 23, no. 3, pp. 740–749, 2016.

[25] F. Schoenbrunn and M. Bach, "The development of paste thickening and its application to the minerals industry; an industry review," *BHM Berg- und Hüttenmännische Monatshefte*, vol. 160, no. 6, pp. 1–7, 2015.

[26] M. Rudman, D. A. Paterson, and K. Simic, "Efficiency of raking in gravity thickeners," *International Journal of Mineral Processing*, vol. 95, no. 1–4, pp. 30–39, 2010.

[27] A. Wu, H. Jiao, H. Wang, S. Yang, G. Yao, and X. Liu, "Mechanical model of scraper rake torque in deep-cone thickener," *Journal of Central South University*, vol. 43, pp. 1469–1474, 2012.

[28] C. K. Tan, J. Bao, and G. Bickert, "A study on model predictive control in paste thickeners with rake torque constraint," *Minerals Engineering*, vol. 105, pp. 52–62, 2017.

[29] S. P. Usher, R. Spehar, and P. J. Scales, "Theoretical analysis of aggregate densification: Impact on thickener performance," *Chemical Engineering Journal*, vol. 151, no. 1-3, pp. 202–208, 2009.

[30] B. B. G. van Deventer, S. P. Usher, A. Kumar, M. Rudman, and P. J. Scales, "Aggregate densification and batch settling," *Chemical Engineering Journal*, vol. 171, no. 1, pp. 141–151, 2011.

[31] H. Wang, X. Zhou, A. Wu, Y. Wang, and L. Yang, "Mathematical model and factors of paste thickener rake torque," *Chinese Journal of Engineering*, vol. 40, pp. 673–678, 2018.

[32] H. Li, H. Wang, A. Wu, H. Jiao, and X. Liu, "Pressure rake analysis of deep cone thickeners based on tailings settlement and rheological characteristics," *Journal of University of Science & Technology Beijing*, vol. 35, pp. 1553–1558, 2013.

[33] S. Yin, A. Wu, K. J. Hu, Y. Wang, and Y. Zhang, "The effect of solid components on the rheological and mechanical properties of cemented paste backfill," *Minerals Engineering*, vol. 35, pp. 61–66, 2012.

[34] W. Sun, A. Wu, H. Wang, T. Li, and S. Liu, "Experimental study on the influences of sodium sulphide on zinc tailings cement paste backfill in Huize Lead-Zinc Mine," *International Journal of Mining and Mineral Engineering*, vol. 6, no. 2, pp. 119–138, 2015.

[35] W. Wang and J. Yang, "Determination of slob-scraper output power of deep-cone thickener and the power check of capacity expansion," *Gold*, vol. 35, pp. 48–50, 2014.

[36] D. R. Kaushal, K. Sato, T. Toyota, K. Funatsu, and Y. Tomita, "Effect of particle size distribution on pressure drop and concentration profile in pipeline flow of highly concentrated slurry," *International Journal of Multiphase Flow*, vol. 31, no. 7, pp. 809–823, 2005.

[37] E. M. Kara, M. Meghachou, and N. Aboubekr, "Contribution of particles size ranges to sand friction," *Engineering Technology & Applied Science Research*, vol. 3, pp. 497–501, 2013.

[38] S. O. Ajamu and J. A. Ige, "Influence of coarse aggregate type and mixing method on properties of concrete made from natural aggregates in ogbomoso oyo state Nigeria," *International Journal of Engineering and Technology*, vol. 5, pp. 426–433, 2015.

[39] A.-X. Wu, Z.-E. Ruan, Y.-M. Wang et al., "Simulation of long-distance pipeline transportation properties of whole-tailings paste with high sliming," *Journal of Central South University*, vol. 25, no. 1, pp. 141–150, 2018.

[40] X. Hui and J. Xie, "Paste technology and its application in tailings treatment," *China Mine Engineering*, vol. 40, pp. 50–54, 2011.

[41] H. Wang, H. Li, A. Wu, and S. Liu, "New paste definition based on grading of full tailings," *Journal of Central South University*, vol. 45, pp. 557–562, 2014.

[42] C. Ince, M. A. Carter, and M. A. Wilson, "The water retaining characteristics of lime mortar," *Materials and Structures*, vol. 48, no. 4, pp. 1177–1185, 2015.